Supplemental Materials fig. s1a (Not to be Published)

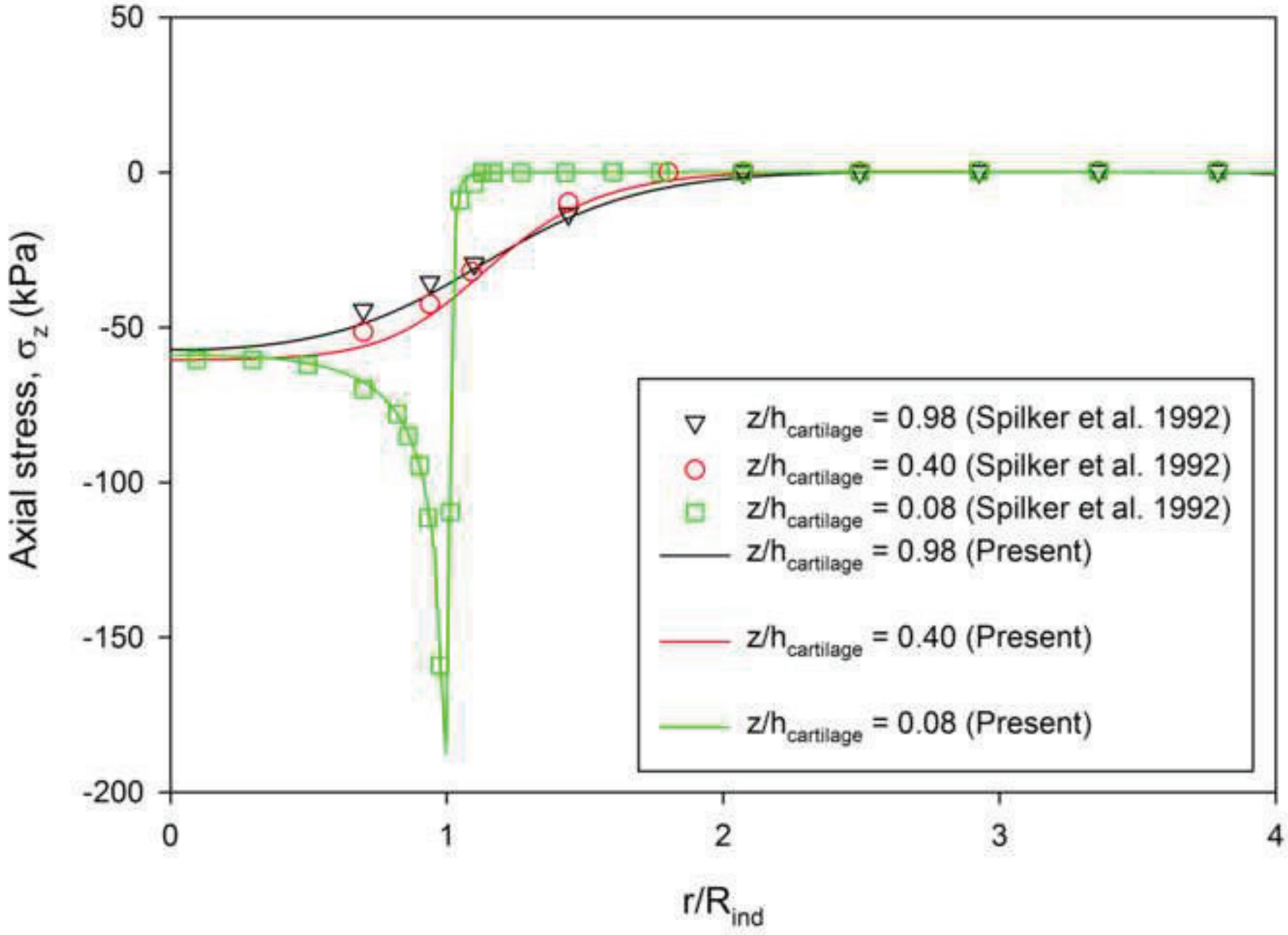

Supplemental Materials fig. s1b (Not to be Published)

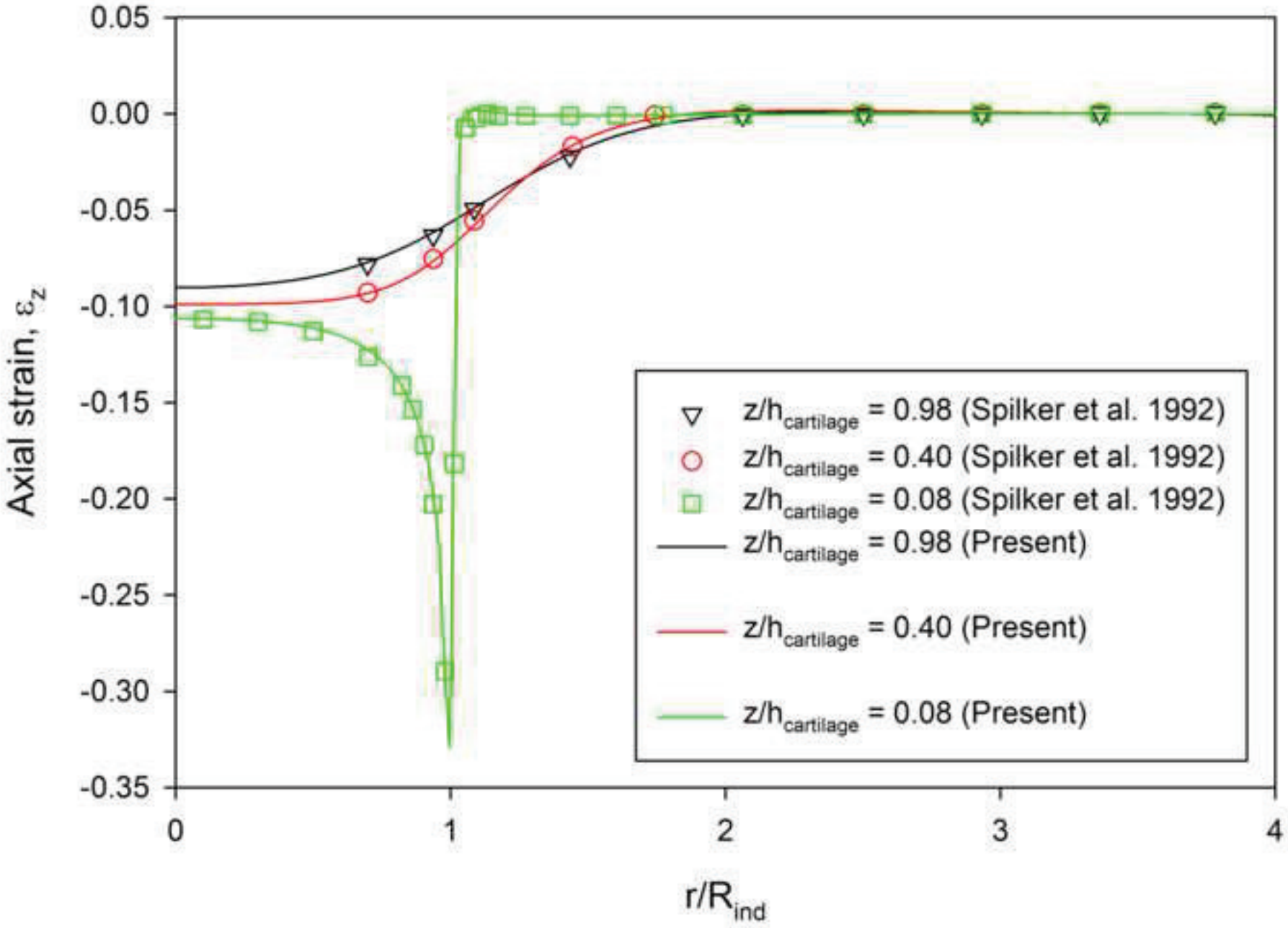

Supplemental Materials fig s1c (Not to be Published)

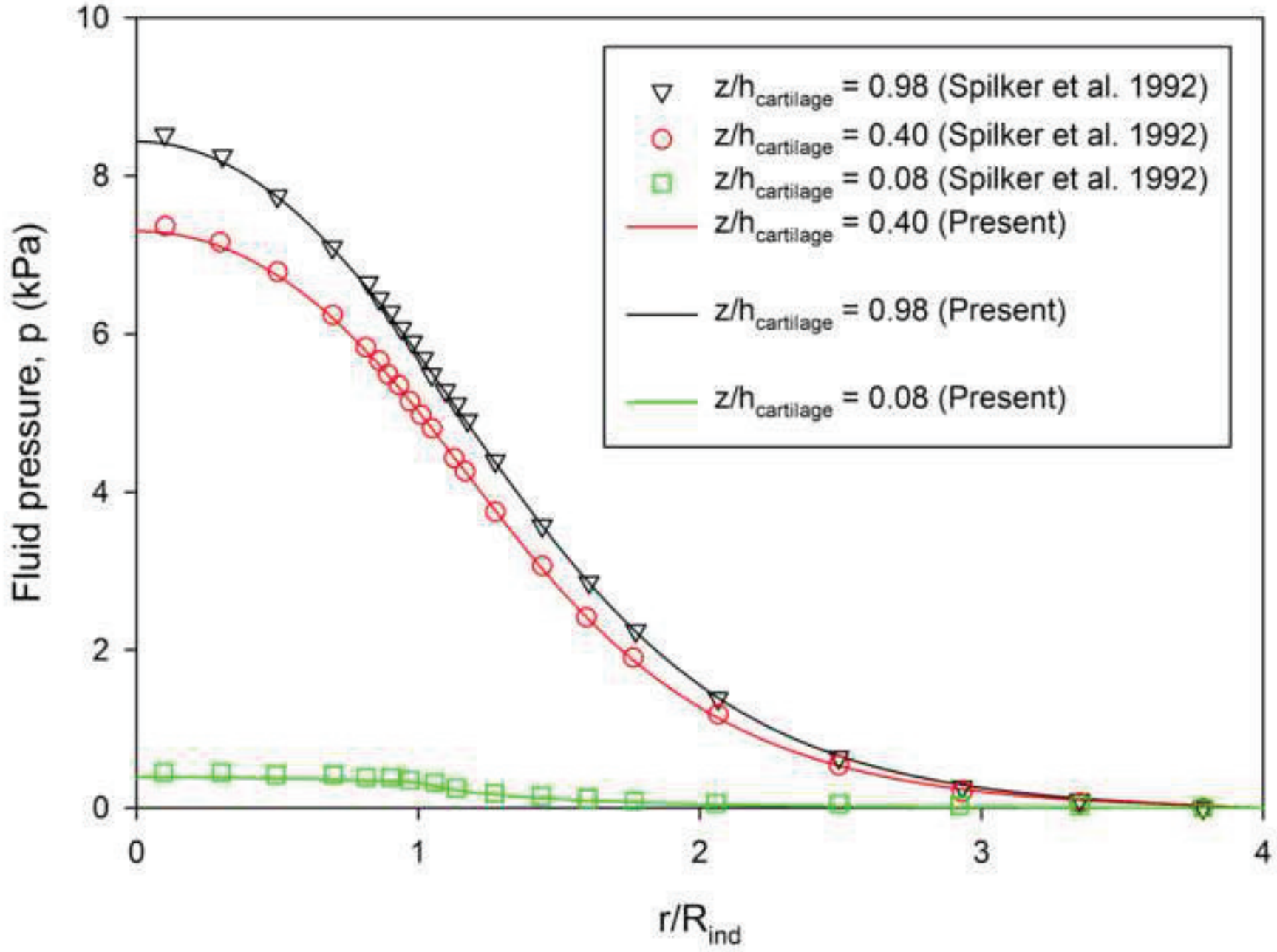

Supplemental Materials table s1 (Not to be Published)

	Young's modulus (MPa)	Poisson's ratio	Permeability ($m^4N^{-1}s^{-1}$)	Solid content
Cartilage	0.5417	0.0833	4×10^{-15}	0.2
Indenter	541.7	0.125	4×10^{-12}	0.95

Supplemental Materials fig. s2 (Not to be Published)

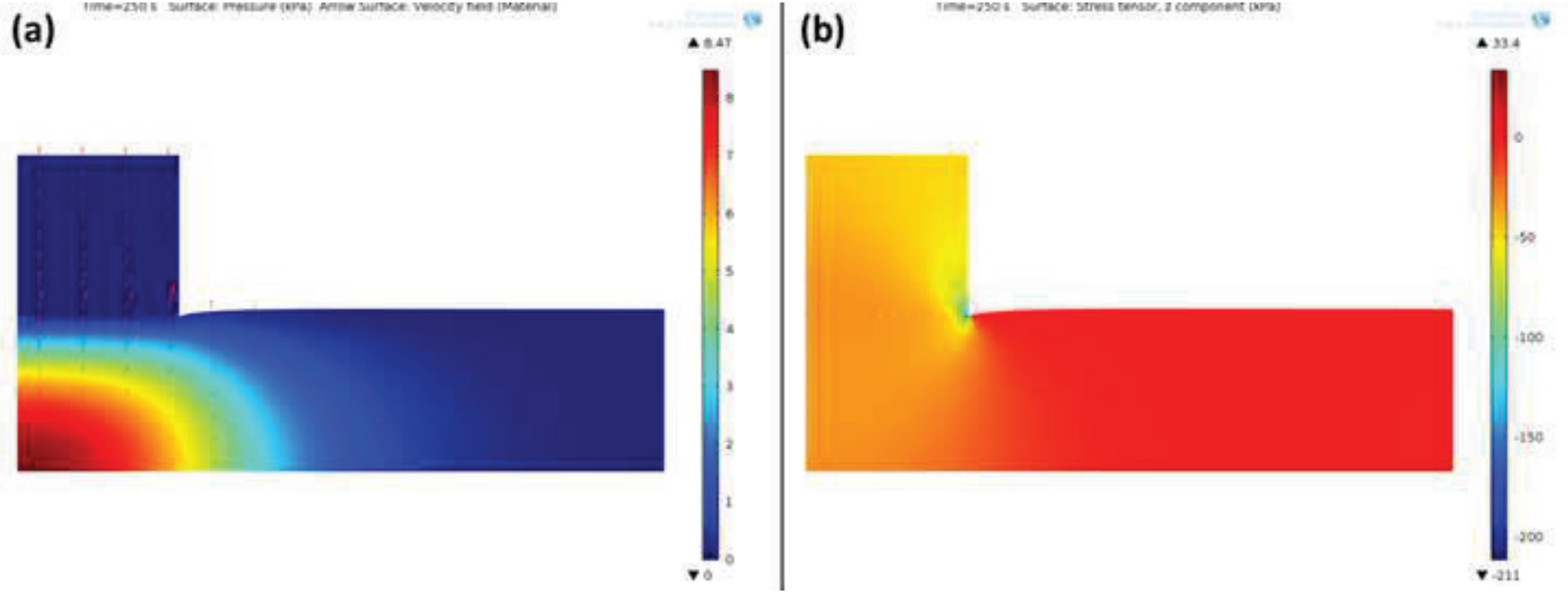

Electronic Supplementary Material

A: MATLAB code for time-delay estimation from pre- and post-compression ultrasonic signals

```
clc
clear all
close all

window_lower=8.0e-6
window_upper=10.0e-6

A =xlsread('pre.csv');    % pre-compression signal
TimeA=A(3:size(A,1)-1,1);
VoltA=A(3:size(A,1)-1,2);
figure(1)
plot(TimeA,VoltA,'b')
hold on
B =xlsread('post.csv');    % post-compression signal
TimeB=B(3:size(B,1)-1,1);
VoltB=B(3:size(B,1)-1,2);
plot(TimeB,VoltB,'r')

VoltA(isnan(VoltA)) = 0;
VoltB(isnan(VoltB)) = 0;
if (TimeA(2)-TimeA(1)) <= (TimeB(2)-TimeB(1)),
    VoltA = interp1(TimeA,VoltA,TimeB,'cubic');   % interp A
```

```
    TimeA = TimeB;
else
    VoltB = interp1(TimeB,VoltB,TimeA,'cubic');    % interp B
    TimeB = TimeA;
end
ind1=find(TimeA<window_lower);
ind2=find(TimeA<window_upper);
VoltA1 = VoltA(size(ind1):size(ind2));
TimeA1 = TimeA(size(ind1):size(ind2));
[val loc] = max(VoltA1(:));
t_ref = TimeA(loc+size(ind1,1)-1)    % peak of uncompressed signal
VoltB(1:size(ind1)-10) = 0;
VoltB(size(ind2)+10:end) = 0;
VoltB(isnan(VoltB)) = 0;
figure(2)
plot(TimeA1,VoltA1,'b',TimeB,VoltB,'r')


X1=normxcorr2(VoltA1,VoltB); %compute cross-correlation between vectors
X1=interp(X1,100);      % upsampling
[m,d]=max(X1); %find value and index of maximum value of cross-correlation
amplitude
dAns = d/100+1-(length(VoltA1)-1);
tShift = (size(ind1,1) - dAns) * (  TimeA(2)-TimeA(1) )
figure(3)
plot(TimeA1-tShift,VoltA1,'b',TimeB,VoltB,'r')
```

B: Finite element analysis.

The finite element model of the three-layered hydrogel construct was verified by comparison with an indentation stress-relaxation model that was developed by Spilker *et al*.[3] In their study, the porous indenter was modeled as a free draining boundary, and the contact between the indenter and the cartilage was not explicitly modeled, but rather compression was applied on the cartilage surface at the indenter site. Later, Guo and Spilker used an augmented Lagrange method to model 2D axisymmetric contact of biphasic cartilage.[2] The algorithm for contact constraints used in the current study differs from that used by Guo and Spilker.[2] A penalty method available in COMSOL Multiphysics (Comsol, Burlington, MA) was used to investigate the frictionless contact mechanics with a poroelastic material. This method can provide faster and smoother convergence but less accuracy of the contact pressure when compared to the augmented Lagrange method. The contact pressure T_n is defined as:[1]

$$T_n = \begin{cases} t_0 - p_n \cdot g & g \le 0 \\ t_0 \cdot \exp\left(-\frac{p_n}{t_0} \cdot g\right) & g > 0 \end{cases} \quad \text{(S1)}$$

where t_0 is an input estimate of the contact pressure, g is the gap distance between the source and destination boundaries, and p_n is the normal penalty factor. In this model for verification, an initial contact pressure is automatically chosen as $t_0 = 1.9 \times 10^3$ Pa by the solver. The default COMSOL expression for p_n is

$$p_n = \frac{E}{h_{\min}} \cdot \min\left(5^k \cdot 10^{-3}, 1\right) \quad \text{(S2)}$$

where E is the Young's modulus of the destination boundary, h_{min} is the minimum mesh size on the destination boundary, and k is the number of iterations in the segregated solver used for analyzing the contact pressure and friction force independently.

An indentation test with a porous indenter was modeled as an axisymmetric problem using the Biot poroelasticity and Darcy's Law to verify the implementation in COMSOL 4.4. In the indentation example of Spilker *et al.*[3] a layer of cartilage of thickness h = 0.75 mm and radius R_0 = 3 mm was indented by a porous flat-ended cylindrical indenter of height h_{ind} = 0.75 mm and radius R_{ind} = 0.75 mm.[2] The ratio of the radii of the cartilage (R_0) to the indenter (R_{ind}) was set at four based on previous results.[3] Cartilage was idealized as a biphasic layer bonded to an impermeable rigid subchondral bone. Spilker *et al.* demonstrated that the inclusion of a deformable subchondral bone layer had an inappreciable effect on the predicted response of the cartilage layer.[3] Therefore, an impermeable fixed boundary condition was imposed along the cartilage-bone interface (at z = 0) instead of explicitly modeling the subchondral bone. A compressive displacement of 0.075 mm, applied on the top of indenter, was increased linearly over 500 s and then held constant. Free-draining boundaries were applied on the top of the indenter (at $z = h + h_{ind}$) and on the cartilage periphery (at $r = R_0$) as well as the surface which was not in contact with the indenter (at $z = h$ and $r > R_{ind}$). Material properties of the cartilage were the same as used in Guo and Spilker (**Table S1**).[2] A contact pair and an identity pair were implemented between the bottom of the indenter and the top of the cartilage. Each pair was composed of a source boundary and a destination boundary. In this case, the bottom of the indenter was defined as the source boundary and the top of

the cartilage was defined as the destination boundary. To improve convergence in the contact model, the mesh on the destination side was finer than that on the source side. Results of our contact solutions (**Figure S1 (a)-(c)**) are in good agreement with those of Spilker *et al.*[3] Near the surface (z/h = 0.98) the axial stress and strain (**Figure S1 (a) and (b)**) drop severely as r/R_{ind} increases, but then quickly rise to zero at the edge of the indenter, r/R_{ind} = 1. In the mid and deeper regions (z/h = 0.4 and z/h = 0.08) axial stress and strain vary smoothly with increasing r/R_{ind}. Fluid pressure is maximum at the center of the model (**Figure S1 (c)**) varies smoothly from the surface and increases with increasing depth. Next, the penalty method for contact constraints used in current study is compared to the augmented Lagrange method used by Guo and Spilker.[2] Distributions of the fluid pressure and axial stress at 250 s (**Figure S2 (A) and (B)**) show qualitative agreement with results of this indentation problem based on the augmented Lagrange method. The pressure distribution is observed to be trivial beyond a radial distance twice the radius of indenter. There is a noticeable difference in axial stress occurring at the edge of the indenter.

Figure Legends

Figure S1 (a): Comparison of the axial stress predicted using the 2D biphasic contact finite element model to that predicted by the 2D biphasic non-contact finite element model of Spilker *et al.*[3] Results are presented at the ramp time of 500 s as used by Spilker *et al.*[3]

Figure S1 (b): Comparison of the axial strain predicted using the 2D biphasic contact finite element model to that predicted by the 2D biphasic non-contact finite element model of Spilker *et al.*[3] Results are presented at the ramp time of 500 s as used by Spilker *et al.*[3]

Figure S1 (c): Comparison of the fluid pressure predicted using the 2D biphasic contact finite element model to that predicted by the 2D biphasic non-contact finite element model of Spilker *et al.*[3] Results are presented at the ramp time of 500s as used by Spilker *et al.*[3]

Figure S2: (a) Distributions of the fluid pressure; red arrows indicate fluid velocity. **(b)** Distribution of axial stress. Both at t = 250s, as used by Spilker *et al.*[3]

Table Legends

Table S1: Material properties for the cartilage and the porous indenter[2] where the value of Young's modulus was also computed from the aggregate modulus and Poisson's ratio found in Spilker *et al.*[3]

References

1. Crisfield M. *Non-linear finite element analysis of solids and structures, Volume 2: advanced topics.* Chichester, England: John Wiley & Sons, Ltd, 1997

2. Guo H. and R. L. Spilker. Biphasic finite element modeling of hydrated soft tissue contact using an augmented Lagrangian method. *Journal of Biomechanical Engineering* 133: 111001, 2011.

3. Spilker R. L., J. K. Suh and V. C. Mow. A finite element analysis of the indentation stress-relaxation response of linear biphasic articular cartilage. *Journal of Biomechanical Engineering* 114: 191-201, 1992.